論 文 の 内 容 の 要 旨

論文題目： Transport phenomena and correlation effects in MgZnO/ZnO interface confined high mobility two-dimensional electron systems

(MgZnO/ZnO界面における高移動度二次元電子の輸送現象と相関効果)

氏 名： ジョセフ リンジー フォルソン

Advances in the field of oxide electronics have accelerated in recent years as a result of technological strides in the controlling the complex chemical and kinetic growth processes. This has delivered many new material platforms with unique degrees of freedom, which have enabled the observation of a wide range of exotic physical phenomenon [1]. A parallel endeavour exists for systems with reduced dimensionality of charge carriers, so called 'two-dimensional' electron systems (2DES). In such systems, an exceptionally rich array of ground states may be observed of both single and many particle origin, such as the integer and fractional quantum Hall (QH) effects [2]. However, such ground states may only be revealed through the understanding and control of the available degrees of freedom, along with the inherent requirement to improve a systems 'quality' so that the effects are not masked by disorder. In this work we report on the development of a new oxide 2DES – that of which is confined at the heterointerface of $Mg_xZn_{1-x}O$ and ZnO, as shown in Fig. 1**a**.

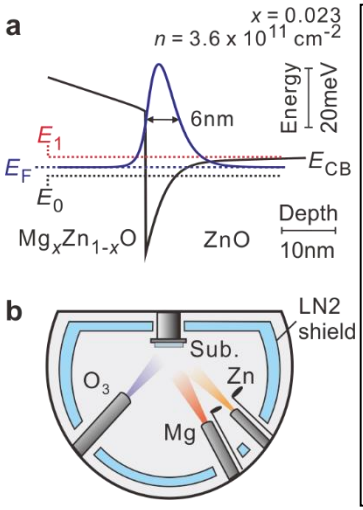

Figure 1: a, Calculations of the quantum well formed in the conduction band (E_{CB}) at the $Mg_xZn_{1-x}O$/ZnO interface. The lowest (E_0) and second (E_1) subbands, along with the Fermi energy (E_F) are indicated. The 2DES occupies only the lowest subband of the quantum well with a wavefunction full-width half-maximum of 6nm (x = 0.023). **b,** Schematic of the MBE apparatus showing the source material cells, substrate, and liquid N_2 shield.

The first achievement of this work is the fabrication of samples comparable to the best semiconductor materials in existence. In order to achieve this, advances in the realm of growth technology have been pursued. In this study, we have developed the oxide molecular beam epitaxy (MBE) technique for the growth of ultra-clean ZnO heterostructures. A schematic of the apparatus is shown in Fig. 1**b**. In addition to high purity Zn and Mg metallic source material, we employ distilled ozone as the oxidizing agent. This has been essential for improving the sample quality, as this greatly reduces the impurity content of films while expanding the possible growth window of coherent epitaxial growth. The heterostructures are grown on single crystal [0001] Zn-polar ZnO substrates and consist of a buffer layer of ZnO and then a capping layer of $Mg_xZn_{1-x}O$. The alloyed x content is known to control the charge density (n) of the system by determining the magnitude of the polarization mismatch (ΔP) at the heterointerface through the relationship $n = \Delta P/e \approx 1.5x \times 10^{13} cm^{-2}$, where e is the elementary charge. In addition to the charge density, the low temperature (T = 500 mK) electron mobility, μ_e, is measured for each sample. This is used to calculate the transport scattering time (τ_{tr}), through $\tau_{tr} = \mu_e m_e^*/e$, where m_e^* is the carrier effective mass. This value is plotted in Fig. 2**a** as a function of density for samples grown during this study after refining the growth conditions (pink[3] and red squares). In this figure we include data for other high mobility 2D materials after scaling with the effective mass. For reference, MgZnO/ZnO heterostructures grown prior to this work using an O_2 radical source for oxidizing species displayed

a peak $\tau_{tr} \approx 25$ ps. The maximum presented in this work is roughly 200 ps, indicating a nearly 10 fold improvement. It can be seen that the red data points which correspond to the ZnO 2DES trail only the GaAs 2DES and 2D hole system (2DHS) in magnitude. In panel **b** we plot the quantum scattering time (τ_q) of charge carriers on the same horizontal axis. This is obtained through an analysis (not shown) of the quantum oscillations in the sample's resistivity in a weak magnetic field. As opposed to τ_{tr} which is weighted towards scattering events with a large change in wavevector, τ_q in theory should be sensitive to all scattering events, and therefore should reflect the true *quality* of a system. By this criteria, the ZnO 2DES remarkably shows quality comparable to state-of-the-art AlGaAs 2DES and 2DHS samples, with scattering times on the order of 15 ps.

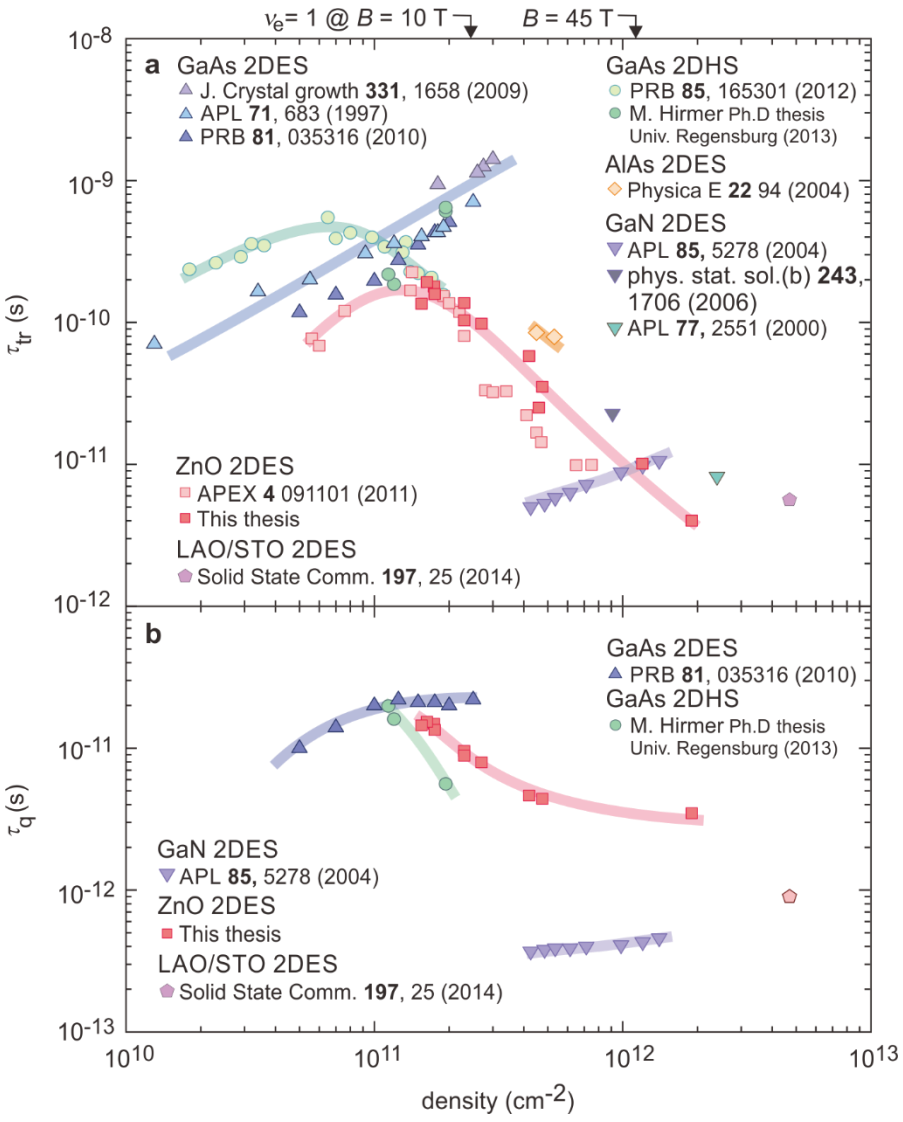

Figure 2: a, Transport scattering time (τ_{tr}) and **b,** quantum scattering time (τ_q) as a function of density for 2D systems including the AlGaAs 2DES and 2DHS, AlAs 2DES, GaN 2DES and $LaAlO_3/SrTiO_3$ 2DES at low temperature. Data are taken from the references noted. On the top axis the B-fields for ν_e=1 are noted (see text).

In 2D systems, by lowering the sample density the strength of electron-electron interaction is enhanced. The parameter that characterizes the strength of the interaction in zero magnetic field is the Wigner-Seitz radius, r_s, defined as the ratio of Coulomb energy to Fermi energy, quantified as:

$$r_s = \frac{E_{coulomb}}{E_F} = \frac{e^2 m_e^*}{4\pi\varepsilon\hbar^2\sqrt{\pi n}} \quad (1)$$

Here, ε is the dielectric constant and $\hbar$ is the reduced Planck constant. Owing to the heavy band mass $m_e^* \approx 0.3m_0$ and small $\varepsilon \approx 8.5\varepsilon_0$ of ZnO, this parameter is naturally higher in comparison with the GaAs 2DES ($m^* \approx 0.07m_0$, $\varepsilon \approx 13\varepsilon_0$), where $r_s \approx 1$. In the highly interacting regime it is both predicted in theory and observed in experiment that 2D systems display renormalization of parameters and may host exotic phase transitions, such as electron crystallization and ferromagnetic instability. These effects may be probed experimentally by reducing n and increasing r_s. This is only possible however in high quality systems where disorder does not overwhelm the conduction of carriers. In Fig. 3**a** we demonstrate a facet of such interaction effects in the MgZnO/ZnO 2DES by showing the spin susceptibility ($g_e^* m_e^*$) of electrons (g_e^* is the g-factor) as a function of n or alternatively r_s (calculated using the band mass). The measurement technique for this is discussed below. With decreasing n, a distinct renormalization of this parameter occurs, with an acute dependence developing for the condition $r_s > 5$.

The spin susceptibility introduced above has a dramatic impact on the highly discretised energy spectrum of allowed states which form the framework for the wide range of ground states observed in 2DES. With the addition of a perpendicular magnetic field, B_p, the constant density of states develops into a ladder of spin split Landau

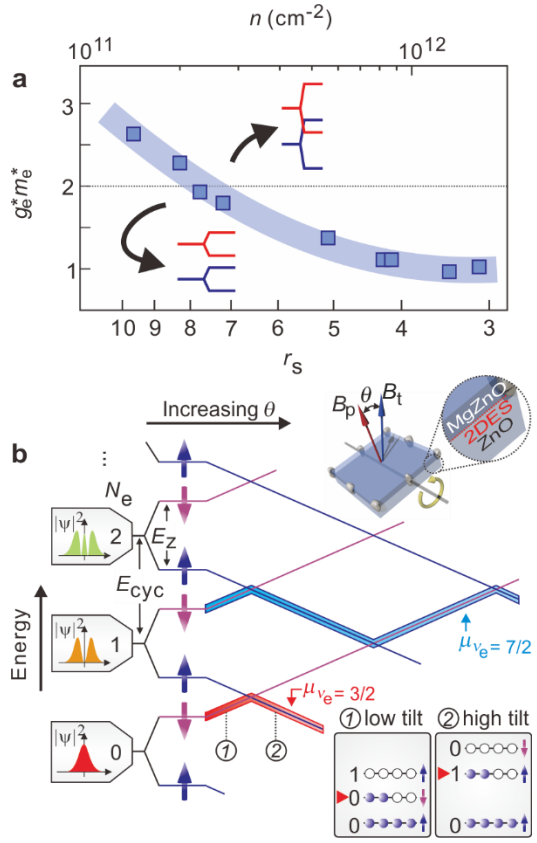

Figure 3: a, $g^*_e m^*_e$ of electrons as a function of n or alternatively, r_s. Spin split LL are shown for the condition of $g^*_e m^*_e$ being larger and smaller than 2. **b**, Electron LL diagram as a function of tilt angle showing multiple crossings. The upper sample schematic shows the experimental geometry. The panels on the left show schematically the differing wave functions between N_e = 0, 1 and 2. Highlighting indicates μ corresponding to ν_e = 3/2 and 7/2 with rotation. The inserts on the bottom right display the level sequence and their quantum numbers on the left and right of the single transition at filling 3/2.

levels (LL) with B_p inducing quantization of the orbital motion and lifting of the spin degeneracy. Each level is characterized by its orbital index N_e = 0,1,… and spin orientation (↓ or ↑), as shown schematically in Fig. 3**b**. As in ZnO there is no valley degeneracy, two 'single particle' energy scales prevail; the Zeman energy E_z ($=g^*_e\mu_B B_t$, B_t is total field and μ_B Bohr magneton) and cyclotron energy E_{cyc} ($=\hbar e B_p/m^*_e$). The spin split LLs energy equals (N_e + ½).E_{cyc} ± E_z/2 with a + (-) sign for spin down (up). Therefore, the condition $g^*_e m^*_e$ = 2 highlighted in Fig. 3**a**, corresponds to when E_{cyc} = E_z, and the ordering of LL swaps spontaneously, as shown schematically. In addition to this, since E_z scales with B_t, while E_{cyc} depends on B_p only, it is possible to swap these levels when rotating the sample relative to the magnetic field, B_t, while maintaining fixed B_p as $B_p = B_t\cos(\theta)$ (see Fig. 3**b** upper insert). Mapping out these crossings enables the quantification of $g^*_e m^*_e$.

Within this picture, each level can host as many charge carriers as magnetic flux quanta thread the sample. The filling factor, $\nu_e = hn/eB_p$, indicates how many levels are occupied and the chemical potential, μ, will shift between LL of different spin orientations and orbital character increasing B_p. When ν_e takes on an integer value, the system goes incompressible and displays the integer QH effect: a Hall resistance R_{xy} quantized in units of $h/e^2\nu_e$, and longitudinal resistance R_{xx} of zero. On the top axis of Fig. 2 we note the magnetic field needed to reach ν_e = 1 for two charge densities. These fields are significant as 10 T may be accessed in a laboratory environment, and 45 T is the maximum static field available today. Therefore, to observe the full spectrum of quantized states, a peak in scattering time at low charge density is highly desirable. This is evidently the case for the MgZnO 2DES. Beyond the integer QH effect which can be conceptualised in terms of single particle energetics, superficially identical behaviour may occur at fractional filling factors in ultra-clean samples. Through the formation of many-body ground states, the fractional QH effect emerges. The vast majority of fractional QH states occur at odd-denominator fillings. This is because the anti-symmetry constraint on the many-particle wave function for Fermions. This is indeed observed in the lowest LL (N_e = 0), where the Coulomb repulsion between electrons is strongest. In contrast, for higher LL ($N_e \geq 2$) the fractional QH effect is altogether absent as charge density wave physics provides energetically more favourable ground states. However, in the second LL (N_e = 1), an *even*–denominator ground state at half filling may occur. The ground state is explained as a paired fluid of quasiparticles called 'composite fermions' and is theorized to be the magnetic field-analogy of a zero-field chiral $p_x + ip_y$ superconductor with excitations who display non-abelian statistics that may have potential applications in fault-tolerant quantum computation[4]. It is thought to emerge at filling 5/2 and 7/2, with these states observed *only* in GaAs 2DES – until now.

Figure 4**a** shows the low temperature (T < 20 mK) magnetotransport of a high mobility MgZnO/ZnO heterostructure. A rich series of integer, along with odd-denominator fractional QH states are observed. Most notably, incipient features of the fractional QH effect are observed at ν_e = 9/2 with robust features at ν_e = 7/2 (panel **b**). A ν_e = 9/2 state has never before been seen, and the ν_e = 7/2 state is the first such observation outside of

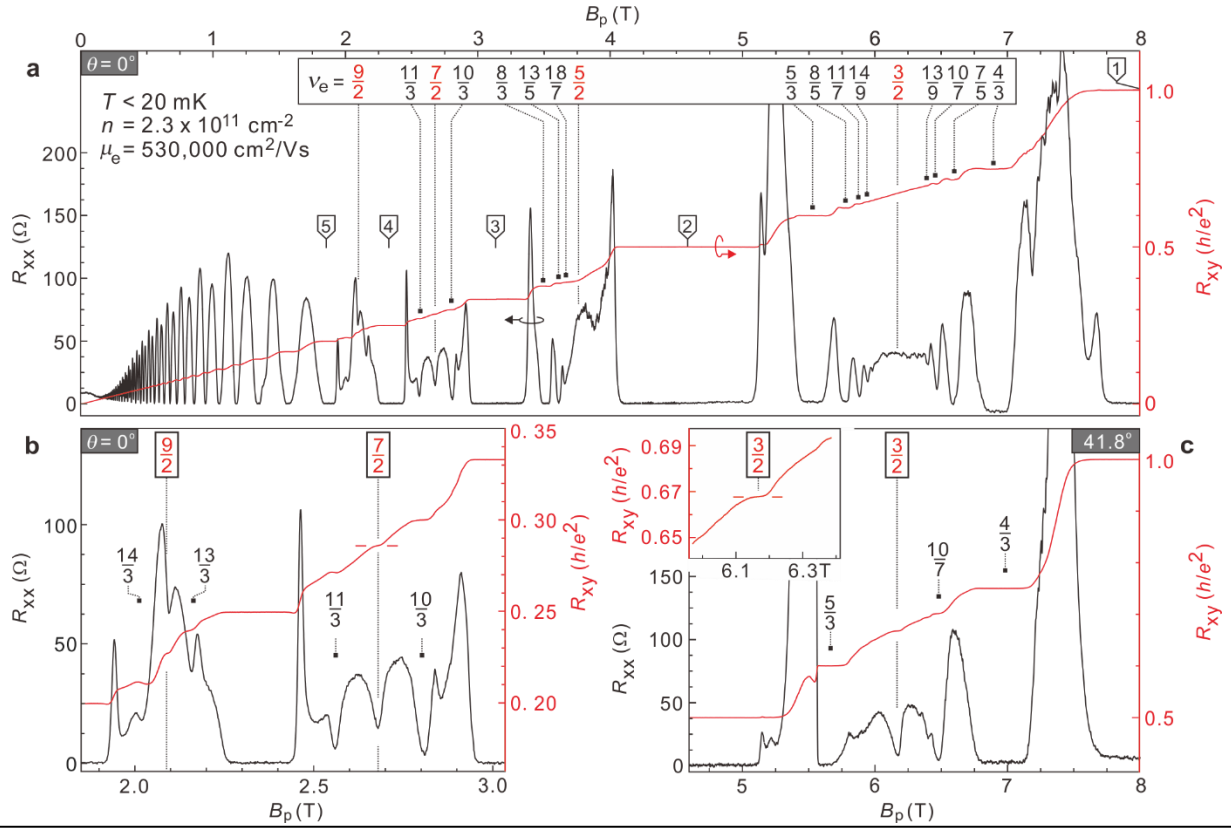

Figure 4: Low temperature (T < 20mK) magnetotransport of a state-of-the-art MgZnO/ZnO 2DES. **a**, A rich series of integer and fractional quantum Hall ground states are indicated. **b**, A zoom in on the region 5 > ν_e > 3 showing incipient features at ν_e = 9/2 and robust features at 7/2. **c**, Transport around ν_e = 3/2 when the sample is titled to 41.8˚ showing a fully developed even-denominator fractional QH state at half-filling.

the GaAs 2DES. However, the most striking facet of the transport is the ability to control the physics of the fractional QH effect through exploiting the spin degree of freedom. As identified above, $g_e^* m_e^*$ is large in the ZnO 2DES and with further enhancement of E_z through rotating the sample, we find it possible to tune the compressible ν_e = 3/2 composite fermion sea into an incompressible fractional QH state when tilting the 2DES from θ = 0º (panel **a**) to ~42º (panel **c**). Observing Fig. 3**b** and the trace corresponding to $\mu_{\nu=3/2}$, it can be seen that at low tilt angles the partially filled level has N_e = 0 character, but this will change to N_e = 1 character after moderate tilting (see right inserts). This is a possible explanation for the appearance of the 3/2 state, as the N_e = 1 LL is known to be able to accommodate an even-denominator ground state. Similarly, for $\mu_{\nu=7/2}$, the partially filled level has N_e = 1 character for zero tilt, but changes with tilt. This is reflected in the transport where the 7/2 state disappears after the first coincidence position at $\theta \sim 25^\circ$ (not shown).

This work establishes the quality of MgZnO/ZnO heterostructures to be on par with the cleanest semiconductor materials in existence. We provide evidence for this through both quantification of scattering rates and the rich array of ground states observed in a magnetic field. Uniquely, this quality occurs concomitantly to the ability to tune to the orbital degree of freedom of partially filled LL, either by modifying $g_e^* m_e^*$ through tuning n or by rotating the sample and forcing level crossings. Using this as an experimental tool, we have demonstrated the discovery of new correlated electron ground states, one of which is an even denominator in the fractional QH state. This realizes a previously unexplored and unique experimental paradigm among low dimensional systems.

[1]H. Y. Hwang, Y. Iwasa, M. Kawasaki, B. Keimer, N. Nagaosa and Y. Tokura, *Nature Materials*, **11**, 103 (2012)

[2]*Perspectives in the Quantum Hall Effects*. Ed. By S. Das Sarma, and A. Pinczuk, (John Willey & Sons, New York, 1997).

[3]J. Falson, D. Maryenko, Y. Kozuka, A. Tsukazaki and M. Kawasaki, *Appl. Phys. Express* **4**, 091101, (2011).

[4]C. Nayak, S. Simon, A. Stern, M. Freedman, and S. Das Sarma, *Rev. Mod. Phys*. **80**, 1083 (2007).